18th IAHR International Conference on Cooling Tower and Air Cooled Heat Exchanger,
16-20 October 2017, Lyon, France

NUMERICAL STUDY OF THE BEHAVIOR OF AN AIR PRE-COOLER

Javier LÓPEZ-NÚÑEZ[1], Blas ZAMORA[1], Antonio VIEDMA[1], Mónica HERNÁNDEZ[1], Francisco SÁNCHEZ[1], Pedro MARTÍNEZ[2], Pedro Juan MARTÍNEZ[2], Javier RUIZ[2], Manuel LUCAS[2] and Antonio S. KAISER[1]

[1]*Universidad Politécnica de Cartagena, Cartagena, Spain*
[2]*Universidad Miguel Hernández, Elche, Spain*

Keywords:Air pre-cooler, Adiabatic cooling pad, Experimental Validation, CFD

ABSTRACT:

Introducing an air pre-cooler step before an air cooler system have been proved to improve the global efficiency of a cooling setup. Several authors have studied the mass and the heat exchanges of an air stream and the water sprayed inside an adiabatic cooling pad. However, these previous studies present their results and correlations as functions of experimental dependent parameters. Therefore, the aim of this study is to develop a numerical modeling capable of characterizing the behavior of an air pre-cooling stage without the need of previous experimental tests, allowing an accurate initial study when designing an air cooler installation.

Several numerical models and simulation tests have been developed by our researching group in order to get a proper approximation of the problem, and the employment of previous experimental data allowed the model validation in terms of pressure drop and air cooling efficiency. As a result, a numerical model is defined, validated, and compared with existing empirical correlations models as a first step to determine the best possible cooling pad configuration in every air cooling setup as a function of the pad geometry, air and water flow rates, with an only numerical simulation.

1 INTRODUCTION

Cooling towers have been widely used for air conditioning in most industries and also in the tertiary sector. Their operating principle requires spraying water on an air stream (Kloppers 2003) which causes the incorporation of water droplets to the air stream and also the release of these droplets to the ambient. This phenomenon is called ‘drift’.

Cooling tower drift must be reduced for several reasons (Lewis 1974). These water droplets may contain chemicals and microorganisms, and they can be released to the atmosphere. The bacteria known as Legionella proliferates in water at the range of temperatures as the frequently found in cooling towers, which make people around the tower vulnerable to inhale aerosols containing the bacteria (Isozumi et al. 2005, Bentham and Broadbent 1993).

Another disadvantage of cooling towers is the restriction that some local Governments apply on their installation after several outbreaks of Legionella. For instance, the local government

of the city of Murcia has forbidden the installation of cooling towers in 2006; in Valencia, there are public aids to replace cooling towers for standard dry coolers in spite of its lower efficiency. This raising in the installation of dry coolers causes the need of investigating alternative ways to improve the efficiency of cooling systems, as long as the air cooler cooling efficiency is lower than the obtained in cooling towers (Pugh 2005); regarding on this, the present study is focused on adiabatic cooling pads, installed as a previous step to air coolers, improving their global cooling efficiency.

Several studies that can be found in the literature have experimentally proved the relations between air temperature decrease, geometrical configuration of the pad and air-water flow ratio. Wind tunnel experimental tests were carried out to define the relation between air flow velocity and cooling efficiency or water evaporation rate, determining correlations for one type of pad (He et al. 2015). Other studies also determined similar correlations through experimental data, (Liao et al. 2002) or (Wu et al. 2009).

Since most of the cited works are based onon previous experimental data for characterizing the cooling pad (He et al. 2014), the present study aims to create a numerical model able to recreate the actual pad behavior, allowing to characterize the cooling pad without the need of experimental tests.This fact will make possible deciding among several types of cooling pads and configurations depending on the requirements of the setup and characterize its behavior. In addition, those different shapes and materials of pads could be tested with this numerical model, as experimentally studied by (Kulkarni and Rajput 2013) for instance.

2 EXPERIMENTAL SETUP

In order to develop an accurate numerical modeling, an experimental validation must be done with previous experimental data from a real installation. An experimental air cooler system was set up in order to study the behavior of its components regarding on the heat and mass exchanges taking place inside (Sanchís 2015). The installation consists of two main coupled parts: air cooler and adiabatic pad. The main elements composing the air cooler are the air vents (which determine the air inlet velocity variable), and the heat exchanger, formed by a set of finned tubes where the water passes through and it iscooled by the air stream (Fig 1).

Figure 1: Experimental cooling pad setup.

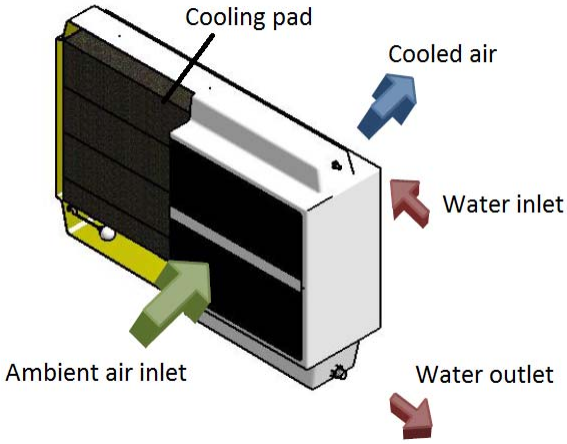

Figure 2: Cooling pad operating scheme.

Regarding on the constructive aspects, the cooling pad is enclosed in a fiberglass structure, forming a tank at the bottom to collect and recirculate the sprayed water by means of a water pump. A set of sprayers are placed at the top of the structure, over the cooling pad, so that the pad is uniformly wet. As a small part of the water evaporates during the process, a water supply pipe is connected to the tank.

The main element of this setup is the pad itself, it consists of a plastic mesh as seen on Fig. 1 and Fig. 2. Its function is to distribute the water uniformly throughout the domain to maximize the air and water contact area. The pad is formed by 500 x 500 mm blocks, completing the whole domain of 2000x1000 mm in frontal area; its thickness is varied by adding more blocks in the air flow direction. Three different types of pad were tested regarding on their compactness; they are named R1, R2 and R3 in this study, whereas their commercial names are RF200, RF240 and RI200 respectively, and their compactness values are 117.2, 140.6 and 234.4 m^2/m^3, respectively (Igual 2014).

Moreover, the adiabatic cooling pad is coupled upstream the air cooler. In this manner, the air stream is forced through the cooling pad, where the water is sprayed to reduce air dry bulb temperature. Water droplets are collected by the pad so that they are not drifted by the air

stream to the downstream heat exchanger, preventing the releasing of harmful microorganisms.

In order to characterize the cooling pad behavior, the cooling efficiency is used as relevant parameter. This variable is useful when comparing different cooling pad operating points or configurations. Cooling efficiency is calculated through several variables that must be measured in the experimental setup.There are the air temperature and the humidity at inlet and outlet sections, as well as the air flow rate from air velocity, and the water flow rate. Fig. 2 shows the operating air and water flows where variables are measured.

3 NUMERICAL MODELLING

3.1 Computational domain and mesh details

The actual evaporative pad has 2000×1000 mm in frontal area, as above mentioned. However, taking into account that the cross-flow pattern of air and water is very similar in each point of the pad, it is possible to consider a reduced domain to study this flow. Firstly, a reduced computational domain consisting of a sample of the whole domain of 50 x 50 mm was studied (Fig. 3), reproducing all the geometrical aspects of the real pad.

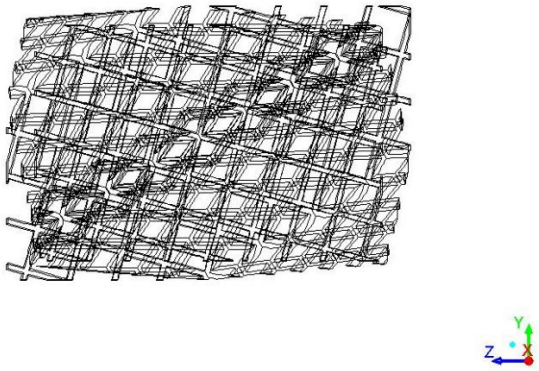

Figure 3: Real pad geometry for the numerical modeling.

Secondly, considering that the basic flow in the domain consists of a cross-flow of air and water around some tubes of “1 mm” diameter, it was studied another simplified geometry composed by a set of parallel and perpendicular tubes arranged on a regular basis (with the same wet area as the actual geometry) and modelling an accurate droplet-pad interaction, as seen on Fig. 4.

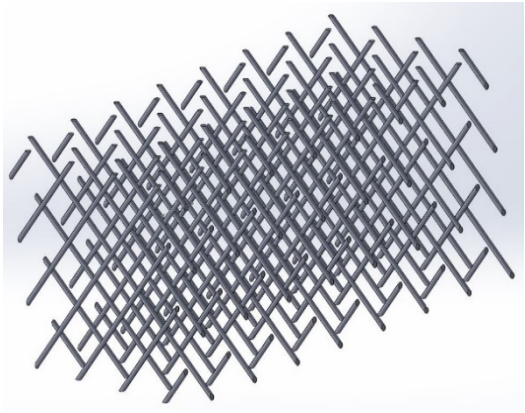

Figure 4: Simplified pad geometry for the numerical modeling.

3.2. Governing equations

In order to model a multiphase flow, aEulerian-Lagrangian approach is used (Patankar and Joseph 2001). It is important to distinguish between the continuous phase, (consisting of the air flow) and the discrete phase (formed by the water droplets), which are considered as solid particles in this type of multiphase flow modelling. Nevertheless, these water droplets can interact with solid surfaces by splashing, spreading or rebounding regarding on the energy droplet impact the wall with.

3.2.1. Air stream equations

The equations for the continuous phase behavior are the following:

$$\frac{\partial(\rho U_j)}{\partial x_j} = 0, \tag{1}$$

$$\frac{\partial(\rho U_i U_j)}{\partial x_j} = \frac{\partial}{\partial x_j}\left[\mu\left(\frac{\partial U_i}{\partial x_j} + \frac{\partial U_j}{\partial x_i}\right) - \frac{2}{3}\mu\left(\frac{\partial U_j}{\partial x_j}\right)\delta_{ij} - \rho\overline{u_i u_j}\right] - \frac{\partial p}{\partial x_i} + \rho g_i, \tag{2}$$

where U is the averaged velocity and p the relative pressure. The term for turbulent stress $-\overline{u_i u_j}$ is obtained from the turbulent closure model, described by

$$-\overline{u_i u_j} = 2\nu_t S_{ij} - \frac{2}{3}k\delta_{ij}, \tag{3}$$

where S_{ij} is the mean strain tensor, $S_{ij} = \left[\left(\partial U_i/\partial x_j\right) + \left(\partial U_j/\partial x_i\right)\right]/2$, δ_{ij} is the Krönecker delta and k the kinetic turbulent energy, given by $k = \sum_{j=1}^{j=3}\overline{u_j^2}\,/2$. The well-know $k-\varepsilon$ turbulence model is employed to solve the closure problem.

3.2.2. Water droplet equations

As described before, water droplets released over the cooling pad from the injectors are considered as particles moving through the pad, impacting over it and interacting with the solid walls of the domain. To solve the trajectories of these particles, the solver uses an integration of the force balance in the particle in a Lagrangian reference frame, equaling the particle inertia with the forces acting on the particle. This can be written as seen in Eq. (4):

$$\frac{du_p}{dt} = F_D\left(U - U_p\right) + \frac{g_i(\rho_p - \rho)}{\rho_p} + F, \qquad (4)$$

where F is an additional acceleration term, and $F_D\left(u - u_p\right)$ is the drag force per unit particle mass. The velocity of the continuous phase is *U,* and U_p is the velocity of the particle, d_p its diameter, and *Re* is the relative Reynolds number, defined in as follows.

$$F_D = \frac{18\mu}{\rho_p d_p^2}\frac{C_D Re}{24} \qquad (5)$$

$$Re = \frac{\rho d_p \left|u_p - u\right|}{\mu} \qquad (6)$$

3.3Solver settings and boundary conditions

The numerical simulations carried out in this work have been solved by using the ANSYS CFD code, based on a finite volume method. In order to simulate the coupling between continuity and momentum equations, the "SIMPLE" algorithm has been used.

There are two different types of cases: the first one simply considers the air flow through the pad; for these cases, the standard *k-ε* turbulence model is employed. A velocity inlet boundary condition is used for the air inlet section, setting just the air velocity magnitude and the turbulence intensity variables; wall conditions are used for the pad tubes and also for top and bottom surfaces, considering that all air exits through the outlet section, where an outflow condition is enabled. Finally, symmetry conditions are chosen for the two sides of the domain.

On the other hand, the other type of case leans on the droplet interaction, and the heat and mass transfer between air and water. In these cases, energy equation and species transport are enabled in order to evaluate the air cooling and water droplet evaporation. Moreover, to simulate water droplets, the Discrete Particle Modeling (DPM) is activated. It is necessary to define the water injections in the top of the domain; water is injected at air wet bulb temperature and at low inlet velocity to approximate the actual droplet behavior. A velocity inlet boundary condition is used for the inlet section, however, as the energy equation and species transport are now activated, the air temperature and the air inlet humidity are also set. Lateral faces continue with symmetry condition; and wall boundary condition is selected for top and bottom surfaces taking into account that DPM particles can escape the domain. At last, for tube walls, the wall film option is enabled, a condition that analyses the droplet impact energy and temperature to evaluate how the interaction between the wall and the droplet will be.

4. EXPERIMENTAL VALIDATION

To characterize and compare numerical and experimental models, the employed variables were the pressure drop and the cooling efficiency. When modelling the pad geometry, reproducing the real pressure drop using the simplified geometry described above was the main goal. Due to the geometry irregularities, the computational modeling behavior must be as similar as possible to the real pad behavior. Pressure drop is one of the selected variables to validate the model because of its clear influence in the setup; in fact, this variable directly affects on the vent consumption, one of the global efficiency factors.

Once pressure drop is validated, the variable that define the similarities between experimental and numerical model in the thermal issue is the cooling efficiency, that can also be validated with the semi-analytical models described by (Wuet al. 2009) or (Liaoet al. 2002).

4.1. Experimental test procedure

In order to get proper experimental data, the cooling pad setup must be previously prepared, that is, cleaning water circuit and prevent any residuals over the pad or the air vents. Once the test begins, water level in the collecting tank must be constant so that water flow rate remains stable during the operation.

Two different types of experimental tests were carried out to get the needed data. On the one hand, pressure drop values were obtained by introducing an air stream through the cooling pad. Air velocity was varied (in the experimental setup) by means of the vent frequency variation, and it was measured at the inlet section of the air pre-cooler, in addition, the air pressure was measured at both sides of the pad, in order to get its evolution. In this way, a relationship between air velocity and pressure drop was obtained.Tab. 1 shows the experimental tests done for pressure drop validation.

Vent Frequency. (Hz)	Air velocity (m/s)			Gauge pressure (Pa)		
	RF200	RF240	RI200	RF200	RF240	RI200
15	1.308	1.194	0.870	4.323	5.236	6.290
20	1.764	1.611	1.213	7.562	8.885	11.190
25	2.313	2.079	1.512	11.838	13.771	17.426
30	2.942	2.489	1.857	16.983	19.571	24.634
35	3.250	3.040	2.241	22.857	26.217	34.158
40	3.695	3.280	2.553	29.534	33.752	43.973
45	4.078	3.861	2.874	37.249	42.435	55.651
50	4.597	4.284	3.148	45.244	51.794	67.515

Table 1: Experimental tests for pressure drop characterization with the three different types of cooling pad.

On the other hand, several tests were carried out injecting water in the setup, so that the cooling pad operates in normal conditions. The measurements were done once the system reached the steady state, when air cooling and tank water level remain constant. These experimental tests were also done with different air velocities, set by varying the vent frequency among 20, 30, 40 and 50 Hz, which means a range of air velocities among 0.6 and 2.2 m/s at the ambient air inlet (Fig. 2). (Igual 2014).A list of some of these experimental tests is shown in Tab. 2, where T1 and T2 are the air temperatures before and after the pad, respectively; Twb is the air wet bulb temperature, V is the air velocity at the inlet, Q is the

water flow rate injected over the pad, H is the air humidity and $\eta$is the cooling efficiency of the cooling pad.

Case		T1 air		T2 air		Twb		V air	Q w	H	η
Pad	Hz vent	(K)	(ºC)	(K)	(ºC)	(K)	(ºC)	m/s	(kg/s)	(kg/kg air)	(%)
R1-80	20	303.32	30.17	299.93	26.78	294.88	21.73	1.07	0.500	0.012840	40.17%
	30	304.48	31.33	300.47	27.32	295.18	22.03	1.73	0.500	0.012796	43.12%
	40	306.01	32.86	300.73	27.58	296.40	23.25	2.04	0.500	0.013974	54.94%
	50	300.96	27.81	298.07	24.92	295.32	22.17	2.16	0.500	0.014473	51.24%
R2-80	20	298.53	25.38	294.44	21.29	291.28	18.13	1.24	0.406	0.010026	56.41%
	30	301.72	28.57	296.41	23.26	292.71	19.56	1.48	0.461	0.010532	58.93%
	40	301.28	28.13	296.61	23.46	293.61	20.46	1.82	0.464	0.011920	60.89%
	50	284.61	11.46	281.46	8.31	279.34	6.19	2.16	0.506	0.003728	59.77%
R3-80	20	303.86	30.71	298.44	25.29	294.71	21.56	1.01	0.456	0.012379	59.23%
	30	303.04	29.89	297.62	24.47	294.17	21.02	1.46	0.472	0.011959	61.10%
	40	304.54	31.39	298.78	25.63	295.31	22.16	1.82	0.500	0.012961	62.41%
	50	302.41	29.26	297.88	24.73	294.90	21.75	1.92	0.456	0.013256	60.32%

Table 2: Experimental tests for cooling efficiency and air temperatures in the pad.

Both types of test were carried out with the three different cooling pad types described above. The compactnessof the R1, R2 and R3 pad types represents the total area of pad material in a cubic meter. Moreover, another pad variable was taken into account, the pad thickness. This variable took values of 80, 160 and 250 mm from the inlet to the outlet section of the cooling pad. Tab. 2 shows the results for the 80 mm pad thickness.

4.2. Pressure drop validation

First numerical simulations were done using the real geometry in order to evaluate the computational cost and time that this geometry implicates. Nevertheless, these results show a poor accuracy compared with the experimental tests, and also the time needed to get them doubled the time needed with simplified geometry numerical tests. It was for those reasons why the real geometry was rejected.

Fig. 5 shows the variation of pressure along the pad, a homogeneous pressure drop is observed in the flow direction. This justify the employment of a reduced section of the whole cooling pad, as long as the behavior of this section represents the whole domain simplifying the computational problem.

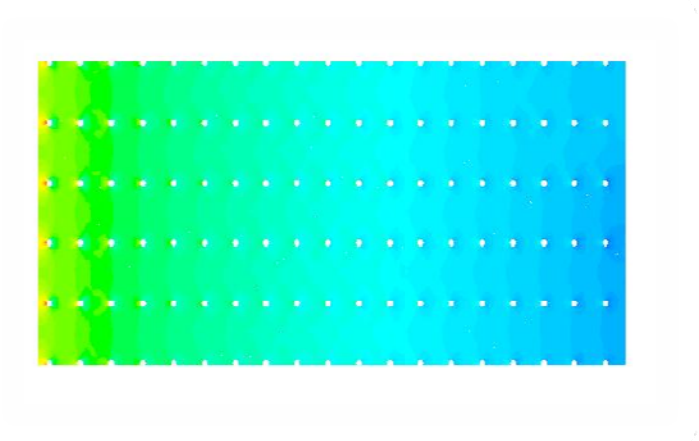

Figure 5: Air pressure drop along the cooling pad.

While real geometry results had a poor quality, the simplified geometry results shown in Fig. 6present a good agreement with the experimental data, for both, the data values as well as the trend of the results.

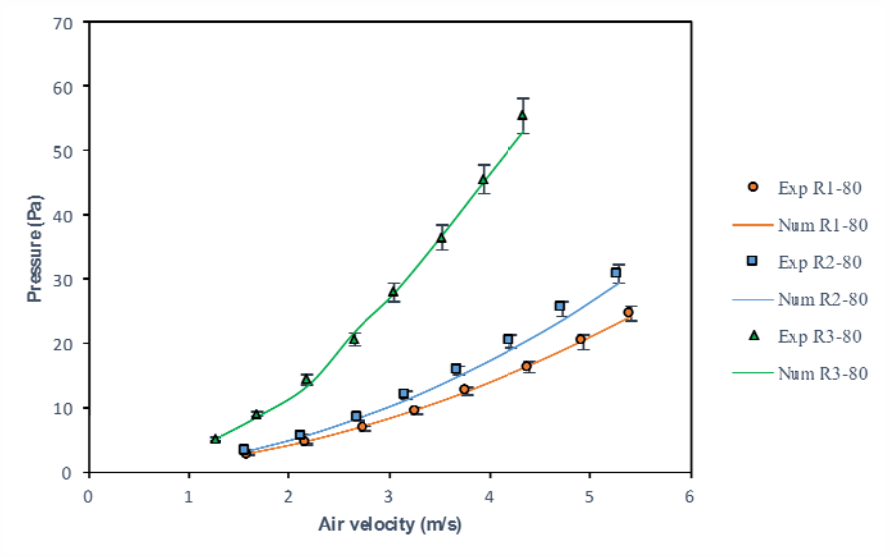

Figure 6: Experimental (Exp) and numerical (Num) results for pressure drop in the cooling pad.

There is a mean error of 1%, meaning that the numerical geometry represents, with quite accuracy, the pressure drop generated by the real cooling pad, as a function of the air velocity. This leads to the next issue of this work, simulating the same geometry including the thermal effects and obtaining results for cooling efficiency.

5. RESULTS AND DISCUSSION

Once the numerical model is validated regarding on the pressure drop across the pad, tests with injected water droplets were carried out following the experimental tests previously done in order to characterize the behavior of cooling efficiency as a function of the problem variables: air and water flow rates, and the geometry variables, thickness and compactness.

5.1. Analytical model comparison

As described in the literature, some analytical models have been developed, characterizing cooling efficiency as a function of air velocity in cooling pads, however, these analytical relations depend on empirical parameters that must be obtained through experimental tests. Nevertheless, these relations are useful in order to check the behavior of our numerical model regarding on the values and trends reached by the cooling efficiency, which is defined as

$$\eta = \frac{t_1 - t_2}{t_1 - t_{wb}} \quad (7)$$

where t_1 is the entering air temperature, t_2 is the air temperature at the outlet section, and t_{wb} is the wet bulb temperature, that is the lowest temperature air could reach as a result of the cooling. This expression, accordingly with (Wu et al. 2009), leads to:

$$\eta = 1 - exp\left(-\frac{h_c \xi \delta}{V \cdot \rho_a c_p}\right) \quad (8)$$

what shows that cooling efficiency is a function of convective heat transfer coefficient between air and waterh_c, the pad geometric characteristicsξ and δ, respectively pad compactness and thickness, air velocity$V$ and the air thermal propertiesc_p. Moreover, this expression may be simplified to:

$$\eta = 1 - exp\left(-\beta \frac{\delta}{V^{\alpha}}\right) \quad (9)$$

where α and β are parameters dependent on geometry of the pad, air thermal properties and h_c, and must be obtained through experimental data, as mentioned before.

To compare numerical model and analytical expressions, these empirical parameters have been set from one of the numerical simulations in order to compare between the trends obtained from numerical and analytical models. Fig. 7 showsthis comparison:

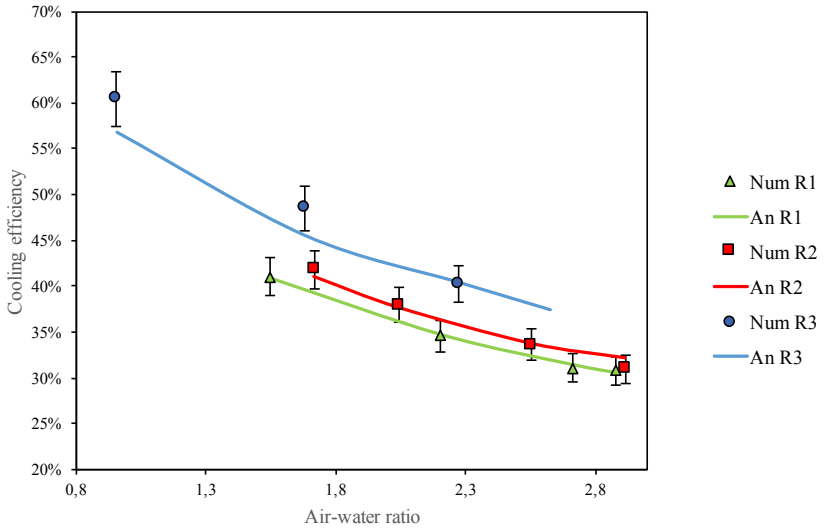

Figure 7: Comparison between the obtained numerical results ('Num' series) and the correlation of Wu et al. (2009) ('An' series).

As it can be observed, both models match accurately, meaning that cooling efficiency calculated from numerical results follow the expected trend. A comparison between numerical simulations and experimental tests will be described in future works.

5.2. Cooling efficiency characterization

As the main result of this study, the relation between cooling efficiency and the rest of problem variables (water an air flow rates, pad thickness and compactness) is described at this point. Once these functions are obtained, the commercial application of the numerical model will lay on the possibility of selecting the type and thickness of cooling pad needed as a function of the setup requirements.

Fig. 8 shows the variation of cooling efficiency as a function of the product of pad thickness and compactness and air-water ratio. As it can be observed, cooling efficiency is higher when the geometrical variable$\xi \cdot \delta$raises, and also when the air/water ratio decreases. These trends can be explained by the fact that the more pad compactness or length, the more heat transfer surface available, what implies a higher air cooling. Moreover, when water flow rate is higher, in relation to air flow rate, there is more water available to exchange heat with the air flow.

As an illustrative example of application of the developed modeling, let us consider a real case in which an installation requires a saturated air stream, the simulation can predict the response of the presented modeling to the calculation of the prescribed air/water ratio for this aim. Fig. 9 shows that at lower air-water ratios, the relative humidity tends towards the saturated state, what could be useful in some applications.

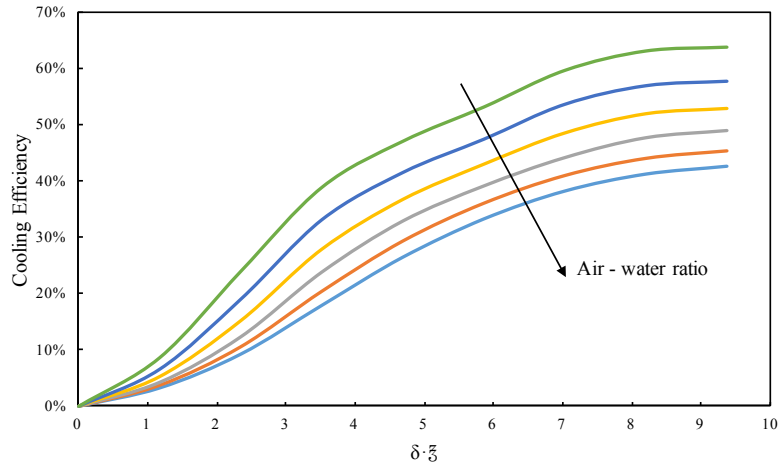

Figure 8. Relation between cooling efficiency and the product of pad thickness and compactness for different air/water ratios.

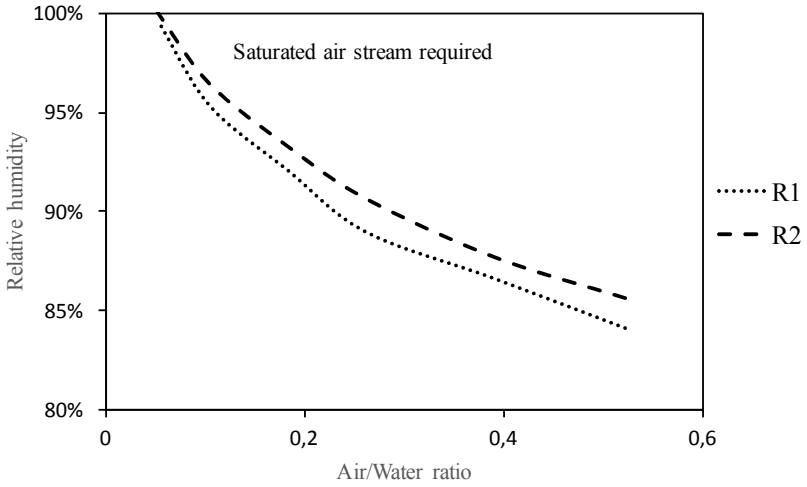

Figure 9. Application example, installation in which a saturated air stream is required.

6 CONCLUSSIONS

In this study, a numerical modeling of a cooling pad behavior installed in an air pre-cooler have been developed. This model has been tested through a CFD code in order to characterize its performance regarding on the pressure drop generated and the air cooling obtained. Two different numerical tests were carried out: the first one was useful to validate the model with the help of previous experimental data from an experimental setup, developed by the same researching group, showing a good agreement. The second type of simulation was employed to define the relations between the cooling efficiency and the problem parameters, determining an improvement in efficiency when air-water ratio decreases, or the product of pad compactness and thickness increases.Moreover, another validation of the numerical model was done, consisting on the comparison with a previous semi-empirical model taken from the literature, showing that trends followed by the cooling efficiency functions, match with the described theoretical trend.

ACKNOWLEDGEMENTS

The authors acknowledge the financial support received from the Spanish Government, through Projects ENE2013-48696-C2-1-R and C2-2-R as well as by the FEDER (*FondoEuropeo de Desarrollo Regional*)

REFERENCES

Bentham R.H, Broadbent C.R, 1993. A model autumn outbreak of Legionnaries' disease associate with cooling tower, linked to system operation and size. *Epidemiol infect.* 111. 287-295.

He S, Zhiqiang G, Gurgenci H,Hooman K, Lu Y, Alkhedhair A, 2014. Experimental study of film media used for evaporative pre-cooling of air. *EnergyConversion and Management*87. 874-884.

Igual A, 2014. Optimización experimental del comportamiento térmico de un aero-refrigerador con pre-enfriamiento adiabático con diferentes espesores de relleno evaporativo. *End of degree project.* UMH, Elche, Spain.

Isozumi R, Ito Y, Osawa M, Hirai T, Takakura S, Iinuma Y, Ichiyama S, Tateda K, Yamaguchi K, Mishima M, 2005. An outbreak of Legionella pneumonia originating from a cooling tower. *Scand J Infect Dis.* 37 (10) 709-711.

Kloppers J. 2003. A critical evaluation and refinement of the performance prediction of wet-cooling towers. *Dissertation for the degree PhD*. University of Stellenbosch, South Africa. December 2003.

Kulkarni R.K, Rajput S.P.S, 2013. Comparative performance analysis of evaporative cooling pads of alternative configurations and materials. *International Journal of Advances in Engineering & Technology.* 6 (4), 1524-1534.

Lewis B.G, 1974. On the question of airborne transmission of pathogenic organisms in cooling tower drift. *Cooling Tower Institute,* Technical paper-T-124A.

Liao C, Chiu K, 2002. Wind tunnel modelling system performance of alternative evaporative cooling pads in Taiwan region. *Building and Environment* 37, 177-187.

Patankar N.A., Joseph D.D., 2001. Modeling and numerical simulation of particulate flows by the Eulerian-Lagrangian approach. *International Journal of Multiphase Flow.* 27 (10), 1659-1684.

Pugh M.D, 2005. Benefits of water-cooled systems vs air-cooled systems for air-conditioning applications. *ASHRAE Expo,* Orlando, USA.

Sanchís J, 2015. Diseño y construcción de un prototipo de Sistema de climatización doméstico con un condensador híbrido empleando un pre-enfriamiento adiabático.*End of degree project.* UMH, Elche, Spain.

Wu J.M, Huang X, Zhang H, 2009. Theoretical analysis on heat and mass transfer in a direct evaporative cooler. *Applied Thermal Engineering.* 29, 980-984.